HIGH EFFICIENCY LARGE AREA POLYSILICON SOLAR CELLS†

S.M. Johnson and C. Winter*

Solarex Corporation, Rockville, Maryland 20850

ABSTRACT

Large area ($100cm^2$) polysilicon solar cells having efficiencies of up to 14.1% ($100mW/cm^2$, 25°C) were fabricated and a detailed analysis was performed to identify the efficiency loss mechanisms. The I-V characteristics of the best cell were dominated by recombination in the quasi-neutral base due to the combination of minority carrier diffusion length and base resistivity. An analysis of the microstructural defects present in the material and their effect on the electrical properties is presented.

INTRODUCTION

Developments in the fabrication of $4cm^2$ single crystal solar cells have yielded efficiencies exceeding 18% under standard terrestrial test conditions [1,2]. More recently, single crystal cell efficiencies exceeding 19% have been reported [3]. In comparison, $4cm^2$ polysilicon solar cells have been fabricated having terrestrial efficiencies up to 17% [4]. Based on these successful results an effort was made to determine the maximum efficiency achievable on large area cast polysilicon material.

MATERIAL AND DEVICE CONSIDERATIONS

Short-Circuit Current

Earlier analyses of short-circuit current limitations in polysilicon solar cells have indicated that for an effective grain diameter (based on electrically active grain and subgrain boundaries) exceeding 1-2 mm, the short-circuit current is essentially determined by the minority carrier diffusion length within the grain volumes [5,6]. Recently it was shown that polysilicon material can be modelled using the concept of an effective minority carrier diffusion length, which depends on the grain diameter and grain boundary surface recombination velocity, incorporated together with single crystal device models [7].

†Work supported by DOE, Cooperative Agreement No. DE-FC01-80ET23197 and by Solarex Corporation

*Current Address: Maryland National Capital Park and Planning Commission

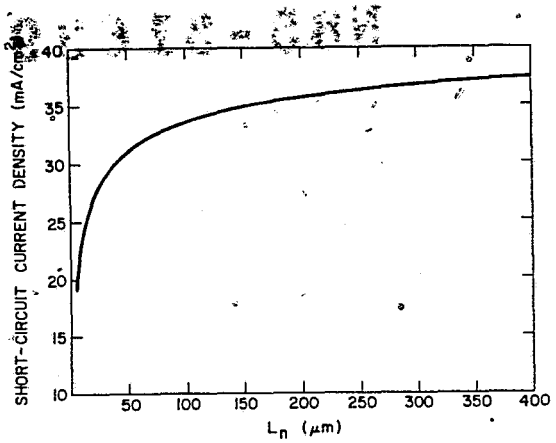

Figure 1. Theoretical Maximum Short-Circuit Current Density Versus Minority Carrier Diffusion Length For a Long-Base Solar Cell ($W >> L_n$), AM1.5, 100mW/cm^2, 400-1100 nm

Figure 1 is a graph of the theoretical maximum obtainable short-circuit current density, in the wavelength range 400 - 1100 nm, versus the minority carrier diffusion length, L_n, in a long-base solar cell (cell thickness W, where $W >> L_n$), calculated using a recently published AM1.5 global spectral irradiance curve (97mW/cm^2) [8]. The calculated values were then increased by 3% to approximate 100mW/cm^2 conditions. Figure 1 shows that for diffusion lengths exceeding approximately 100 μm, in a long-base solar cell, the short-circuit current increases asymptotically with increases in diffusion length. For an effective grain size of 1-2 mm, intragrain diffusion length of 250 μm, and an infinite grain boundary surface recombination velocity, the effective diffusion length in polysilicon material would be approximately 120 - 170 μm and grain boundary effects on short-circuit current are minimal [7].

The material used in this study has average grain diameters of 2 - 10 mm, however the presence of dislocation subgrain boundaries within some of the large grains locally reduces the effective grain size and the effective minority carrier diffusion length. A detailed study of the origins and electrical properties of subgrain boundaries in cast polysilicon material has been performed [9]. For typical subgrain diameters in the range 0.1 - 0.3 mm the effective diffusion length can be reduced to 40 - 90 μm, using the previous values of intragrain diffusion length and surface recombination velocity, and reduce the short-circuit current [7]. A decreased effective lifetime in regions containing subgrain boundaries, revealed using a Secco etch, has been reported earlier [10]. Thus it is important to obtain polysilicon material which has a long intragrain diffusion length and has a minimum density of subgrains.

Open-Circuit Voltage and Fill Factor

Neglecting series resistance and shunt conductance the dark I-V characteristics of a solar cell can be written as

$$J_d = J_{sco}[\exp(qV/nkT)-1] + J_{qno}[\exp(qV/kT)-1] \qquad (1)$$

where the first term is the current component arising from recombination in the space-charge region (with a diode ideality factor, n) and the second term is the current component due to recombination in both the quasi-neutral emitter and quasi-neutral base of the solar cell [11]. With the use of single crystal base material and high quality, careful, cell processing, the space-charge component is usually negligible.

In order to maximize the open-circuit voltage most workers have first minimized the quasi-neutral base recombination component by using boron-doped, high lifetime, low resistivity (0.1-0.3 Ω-cm) float-zoned single crystal silicon as a base material and then minimized the quasi-neutral emitter recombination by a combination of tailoring the emitter doping profile and/or passivating the surface with a thermally grown oxide [12-17,2]. The most successful work to date is the MINP solar cell design [18-19].

Empirically it has been found in the past that the minority carrier diffusion length in cast polysilicon material decreases rapidly for base resistivities below approximately 1 Ω-cm and that good quality material can be grown in the 1-2 Ω-cm resistivity range. Thus in order to apply these results the recombination current in the quasi-neutral base must first be estimated for this range of base resistivity. The quasi-neutral base recombination current, J_{qno}, can be calculated for two different conditions [14], (1) the long-base solar cell ($W>>L_n$):

Long-base
$$J_{qno} = \frac{qn_i^2 D_n}{N_A L_n} \qquad (2)$$

and (2) the perfect back surface field (BSF) condition (back surface recombination velocity is zero):

BSF
$$J_{qno} = \left(\frac{qn_i^2 D_n}{N_A L_n}\right) \tanh(W/L_n) \qquad (3)$$

where q is the electronic charge, n_i is the intrinsic carrier concentration, D_n is the minority carrier diffusivity, N_A is the base doping concentration, L_n is the minority carrier diffusion length and W is the base thickness. Using Figure 1, and equations (2) and (3) the maximum, base-limited, open-circuit voltage under 100mW/cm^2, 25°C conditions was calculated as a function of minority carrier diffusion length for ρ = 1 Ω-cm, W = 150 μm and ρ = 1.7Ω-cm, W = 225 μm, and is shown in Figure 2. These resistivity/thickness combinations correspond to base parameters for a high efficiency 4cm^2 and the 100cm^2 polysilicon solar cells respectively discussed later.

Figure 2 shows that for a 1 Ω-cm, 150 μm thick cell the minority carrier diffusion length must be, for a base-limited open-circuit voltage to exceed 600mV, greater than 170 μm for a BSF cell and greater than 240 μm for a long-base cell. For a 1.7 Ω-cm, 225 μm thick base the minority carrier diffusion length must be greater than 300 μm for a BSF cell and greater than 400 μm for a long-base cell. Thus, the use of high base resistivity material puts a large lower limit on the range of the minority carrier diffusion length necessary to reach a base-limited open-circuit voltage of 600 mV and places further emphasis on obtaining material with a minimal lifetime inhomogenity. It was recently demonstrated experimentally that reduced open-circuit voltages in large-grained polysilicon solar cells were due to a lower minority carrier diffusion length in the base substrate material [20]. As discussed previously, the effective minority carrier diffusion length in regions containing subgrain boundaries can be as low as 40-90 μm. In these localized regions, using Figure 2, the open-circuit voltage can range from 550 - 575 mV for 1 Ω-cm material and from 530 - 550 mV for 1.7 Ω-cm material. Open-circuit voltage degradation due to increased quasi-neutral base recombination associated with

subgrain boundaries was recently reported [21]. In order to estimate areal inhomogenity effects the I-V characteristics of a large area cell can be obtained by summing the short-circuit and dark current components from the different regions of the cell in parallel.

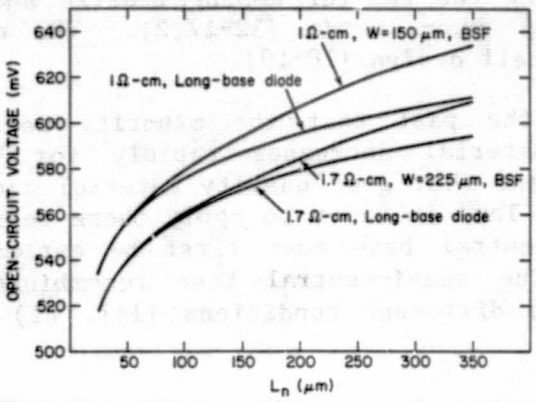

Figure 2. Theoretical Maximum, Base-Limited, Open-Circuit Voltage Versus Minority Carrier Diffusion Length for Various Base Parameters, 100mW/cm^2, 25°C

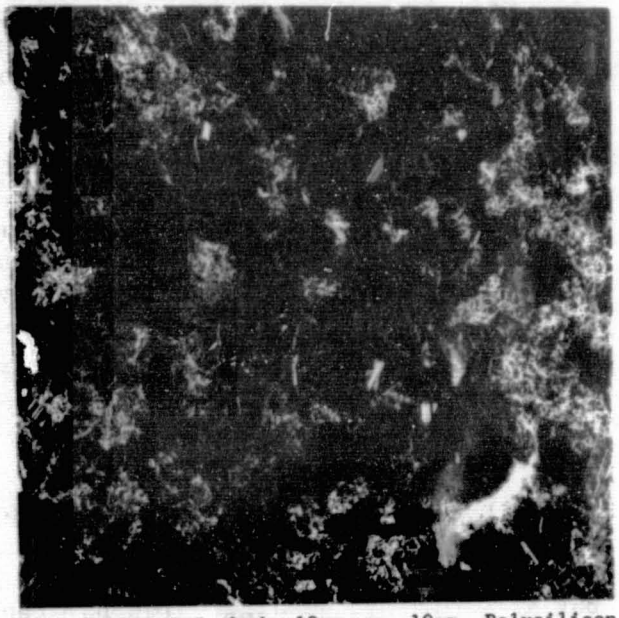

Figure 3. Secco-Etched 10cm x 10cm Polysilicon Wafer Serial Section

In order to minimize recombination in the base material, wafers were selected on a basis of having a reasonably long decay time, proportional to the free-carrier lifetime, measured with a contactless modulated microwave reflectance technique [10] and having a minimal number of subgrain boundaries. Figure 3 shows a photograph of a Secco-etched 100cm^2 polysilicon serial section used in this effort and Figure 4 is a micrograph of a typical region containing subgrain boundaries with spacings of 0.1 - 0.5 mm. Subgrain boundaries have always been found to cause minority carrier recombination as seen in both fine light spot scanning [10] and EBIC [9] measurements. It was estimated by inspection of the Secco-etched 100cm^2 wafer that approximately 8% of the total wafer surface is comprised of regions similar to Figure 4.

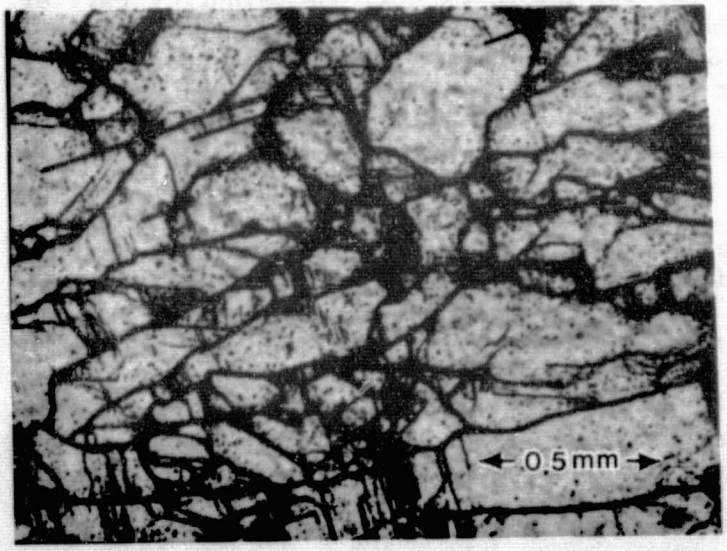

Figure 4.
Micrograph Showing A Dense Array of Subgrain Boundaries

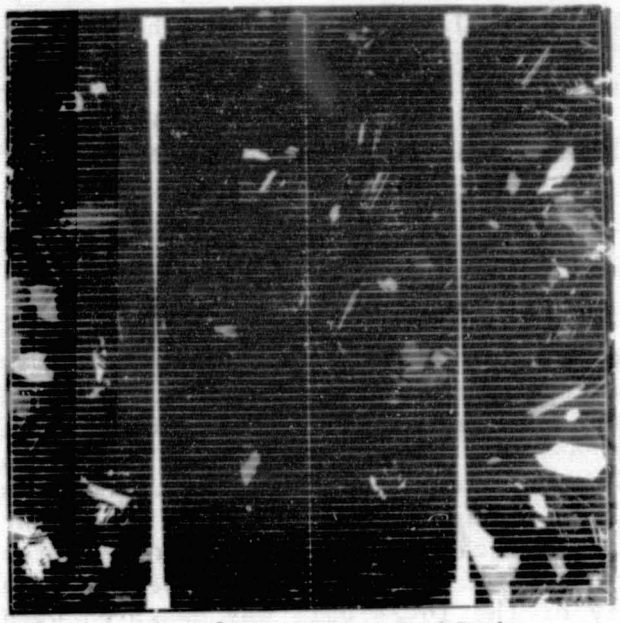

Figure 5. 100cm^2 Cell Showing Grid Design

CELL AREA (cm^2)	NO. CELLS	STATISTIC	J_{sc} (mA/cm^2)	V_{oc} (mV)	F.F.	EFFIGIENCY (%)
100	50	MEAN	30.6	574	0.761	13.4
		σ	0.66	5.9	0.011	0.31
100	1	-	31.3	584	0.771	14.1
4.03	1	-	34.6	601	0.779	16.2

Table 1. Polysilicon Solar Cell Illuminated I-V Characteristics (100mW/cm^2, 25°C)

Although recombination in the space-charge region is normally negligible in single crystal silicon solar cells, it can, if present, seriously reduce the fill factor and open-circuit voltage. Increased space-charge recombination is associated with subgrain boundaries in polysilicon solar cells and has the largest influence on fill factor rather than open-circuit voltage [21]. Thus there was a further reason to minimize the area of such regions in a large area polysilicon solar cell.

CELL FABRICATION AND RESULTS

A total of fifty 100cm^2 cells were fabricated using space-quality cell processing technology. The p-type wafers were thinned to a nominal thickness of 225 μm using a CP etch and then given a short etch in NaOH to yield a slightly textured surface. (Although a further reduction in thickness would allow for a more beneficial BSF effect, the difficulty in processing a 100cm^2 wafer thinner than approximately 225 μm was too great for the scope of the experiment.) The wafers were then phosphorus diffused to a sheet resistance of approximately 100 Ω/□; aluminum paste was screen printed, alloyed, and the residual paste was removed with HCl. Contacts were photolithographically defined and the metallization consisted of evaporated/ electroplated Ti/Pd/Ag. Figure 5 is a photograph of a 100cm^2 cell showing the grid metallization design. Four buss conductors were used to help minimize the metallization shadowing. A two-layer evaporated antireflection coating was applied, consisting of Ta_2O_5 as the first layer and MgF as the second layer, followed by a brief sintering step.

The short-circuit current was measured outdoors at 100mW/cm^2 illumination, referenced to a global pyranometer measurement (Eppley PSP), and the I-V curves were then completed on a filtered xenon simulator at 25°C. The average and standard deviation of the illuminated I-V characteristics of the fifty cells is given in Table 1. These cells had an average efficiency of 13.5% and

the best cell had an efficiency of 14.1%. Table 1 also summarizes the illuminated I-V characteristics of the best large area cell together with the characteristics of a small area ($4.03cm^2$) 16.2% efficient polysilicon solar cell fabricated during an earlier study [4]. The efficiency of the small area polysilicon solar cell was independently confirmed at the Solar Energy Research Institute [22].

ANALYSIS

Short-Circuit Current

In order to quantify the efficiency loss mechanisms, a detailed loss analysis of the best large area cell together with a high efficiency small area cell was performed. Figures 6 and 7 show the internal and external quantum efficiencies of the 16.2%, $4.03cm^2$ cell and the 14.1%, $100cm^2$ cell respectively in the wavelength region 400 - 1100 nm. Of particular note is that both cells exhibited a spectral response which varied with light intensity [23]. The observation of a minority carrier diffusion length which is dependent on injection level has been studied previously in other silicon materials [24,25]. The quantum efficiency of the 16.2% cell was measured with a chopped monochromatic beam and a steady white light bias of approximately 1 sun intensity [23]. The large area cell was measured with a white light bias of approximately 0.1 sun bias intensity due to measurement limitations. Thus, although it is possible that the near infrared quantum efficiency measured for this cell is inaccurate, no significant variation was found in the range of 0.05 - 0.1 sun bias indicating that the traps dominating the low injection lifetime were saturated.

Figure 8 shows the internal quantum efficiency measured, at approximately 1 sun bias, in a region containing subgrain boundaries and an adjacent region free of subgrain boundaries (both regions are in the 14.1%, $100cm^2$ cell). The effective minority carrier diffusion length in the subgrain region was calculated from the linear plot of inverse quantum efficiency versus inverse absorption coefficient [26] to be 80 μm. This value is approximately one-third of the base thickness so that ignoring BSF effects in the diffusion length calculation is justified. In contrast, a calculation of the diffusion length in the subgrain-free region, or for the curves in Figure 6 and 7 using this method yields diffusion length values close to or exceeding the base thickness. Thus the analysis assumptions are violated and these values are inaccurate.

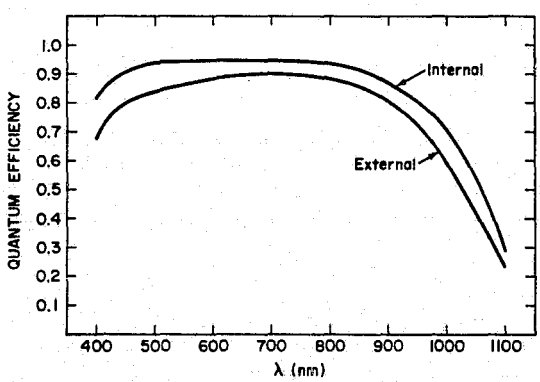

Figure 6. Internal and External Quantum Efficiency Versus Wavelength For the 16.2%, $4.03cm^2$ Polysilicon Solar Cell (∿ 1 sun bias condition)

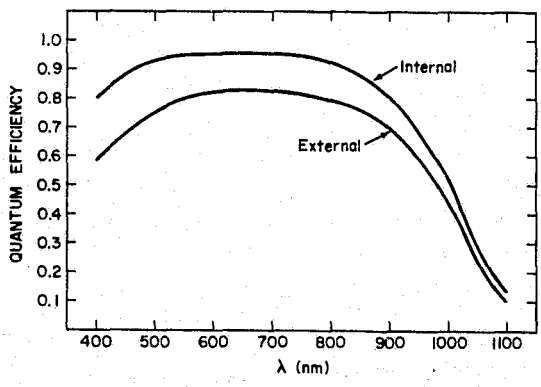

Figure 7. Internal and External Quantum Efficiency Versus Wavelength For the 14.1%, $100cm^2$ Polysilicon Solar Cell (∿ 0.1 sun bias condition)

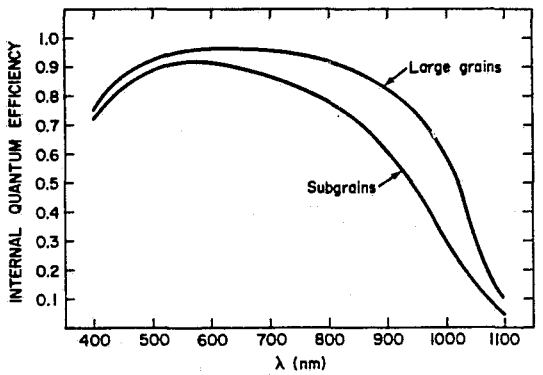

Figure 8. Internal Quantum Efficiency in Large-Grain and Subgrain Regions of the Large Area Polysilicon Solar Cell (∿ 1 sun bias condition)

	16.2% (4.03cm²)		14.1% (100cm²)	
LOSS MECHANISM	FRACTION AVAILABLE AFTER LOSS	J_{sc}(mA/cm²) AVAILABLE AFTER LOSS	FRACTION AVAILABLE AFTER LOSS	J_{sc}(mA/cm²) AVAILABLE AFTER LOSS
THEORETICAL MAXIMUM	1.0	43.2	1.0	43.2
INTERNAL QUANTUM EFFICIENCY LOSS	0.87	37.6	0.85	36.7
ANTIREFLECTION COATING LOSS	0.97	36.5	0.97	35.6
GRID SHADOWING LOSS	0.95	34.6	0.88	31.3
NET	0.80	34.6	0.73	31.3

Table 2. Short-Circuit Current Losses for the Small and Large Area Polysilicon Cells in the Region 400 - 1100 nm

By separately integrating the product of each quantum efficiency curve with the AM1.5 solar spectral irradiance curve [8] over the wavelength range 400 - 1100 nm, and by measuring the percentage grid shadowing, the percent losses in short-circuit current due to internal quantum efficiency, anti-reflection coating, and grid shadowing were calculated. This short-circuit current loss analysis is summarized in Table 2. The short-circuit current associated with the internal quantum efficiency of the small area cell is approximately 2% greater than the large area cell partly due to a reduced cell thickness (150 μm versus 225 μm), which enhances BSF effects, and the addition of a back-surface reflector (BSR) which was not used for the large area cells. From an analysis of Figure 8 a total internal quantum efficiency loss in short-circuit current of only approximately 1% can be attributed to the 8% area of the cell containing subgrain boundaries. Antireflection coating losses were identical. The major difference between the two cells was the percentage of grid shadowing, representing approximately 5% for the small area cell and 12% for the large area cell. The grid shadowing is approximately twice the design value for the large area cell and was due to excessive grid line broadening during the photolithography and metallization processes.

Open-Circuit Voltage and Fill Factor

The dark I-V characteristics of both cells were generated by measuring I_{sc}-V_{oc} at different illumination levels to eliminate the effect of series resistance and then subtracting the shunt conductance contribution (determined from reverse-bias measurements). This data was then fitted to equation (1) using a computer program designed to minimize the differences between the measured data and the I-V characteristics calculated from equation (1) [27]. The series resistance was calculated from the difference in the I_{sc}-V_{oc} and dark forward-bias I-V characteristics. The base resistivity was calculated from junction capacitance measurements. These results are summarized in Table 3.

Using the shifting approximation, the illuminated I-V characteristics were calculated from the short-circuit current and dark I-V characteristics in Table 3. This calculation was done by starting with the quasi-neutral component alone, calculating the illuminated I-V characteristics, and then sequentially adding the space-charge component, shunt conductance, and series

PARAMETER	16.2% (4.03cm²)	14.1% (100cm²)
SHUNT CONDUCTANCE G(mV/cm²)	0.18	0.90
SERIES RESISTANCE R_s(Ω-cm²)	0.38	0.32
SPACE-CHARGE DIODE QUALITY FACTOR, N	3.5	2.0
SPACE-CHARGE CURRENT J_{sco}(mA/cm²)	4.6×10^{-3}	6.3×10^{-4}
QUASI-NEUTRAL CURRENT J_{QNO}(mA/cm²)	2.3×10^{-9}	3.6×10^{-9}
EQUIVALENT VOLTAGE V_E(mV)	522	496
BASE RESISTIVITY (Ω-cm)	1.0	1.7

Table 3. Dark I-V Characteristics for the Small and Large Area Polysilicon Solar Cells

INCLUDED DARK I-V COMPONENTS	I-V CHARACTERISTICS CALCULATED FROM INCLUDED DARK I-V COMPONENTS			
	V_{oc} (mV)	F.F.	η (%)	Δη (%)
QUASI-NEUTRAL RECOMBINATION	602	0.829	17.2	-
QUASI-NEUTRAL & SPACE-CHARGE RECOMBINATION	599	0.796	16.4	0.8
QUASI-NEUTRAL, SPACE-CHARGE & SHUNT CONDUCTANCE	599	0.793	16.4	0
QUASI-NEUTRAL, SPACE-CHARGE, SHUNT CONDUCTANCE & SERIES RESISTANCE	599	0.775	16.1	0.3
MEASURED CHARACTERISTICS	601	0.779	16.2	-

TABLE 4A

INCLUDED DARK I-V COMPONENTS	I-V CHARACTERISTICS CALCULATED FROM INCLUDED DARK I-V COMPONENTS			
	V_{oc} (mV)	F.F.	η (%)	Δη (%)
QUASI-NEUTRAL RECOMBINATION	588	0.826	15.2	-
QUASI-NEUTRAL & SPACE-CHARGE RECOMBINATION	584	0.803	14.7	0.5
QUASI-NEUTRAL, SPACE-CHARGE & SHUNT CONDUCTANCE	583	0.791	14.4	0.3
QUASI-NEUTRAL, SPACE-CHARGE, SHUNT CONDUCTANCE & SERIES RESISTANCE	583	0.777	14.2	0.2
MEASURED CHARACTERISTICS	584	0.779	14.1	-

TABLE 4B

Table 4. Illuminated I-V Losses Calculated Using the Shifting Approximation and the Dark I-V Characteristics in Table 3 for the Small Area (Table 4A) and Large Area (Table 4B) Polysilicon Solar Cells

resistance, and repeating the calculation after each addition. Table 4A summarizes the results of this calculation for the 16.2% small area cell. Space-charge recombination reduced the open-circuit voltage minimally (∿3 mV), however it caused a 0.8% reduction in cell efficiency (17.2 to 16.4%) due to a decreased fill factor. The cause of this increased space-charge component was not identified. The shunt conductance was sufficiently low to not affect the cell efficiency, however series resistance decreased the fill factor and caused a 0.3% reduction in cell efficiency. The uppermost curve in Figure 2 shows that, theoretically, the open-circuit voltage of a perfect BSF cell of this thickness and base resistivity must have a base minority carrier diffusion length exceeding approximately 180 μm, which may be possible, in order to achieve a base-limited open-circuit voltage larger than experimentally obtained. The base diffusion length and back surface recombination velocity are difficult parameters to measure in a BSF cell and were not measured in this study. (Techniques to separately determine the base and emitter dark current components have been recently reported [28,29]). However, based on the above analysis of the dark current and Figure 2, the open-circuit voltage of the 16.2% cell is approaching the level where recombination in the quasi-neutral emitter begins to dominate.

Table 4B summarizes the calculated I-V characteristics of the 14.1% large area cell. Space-charge recombination again reduced the open-circuit voltage minimally (∿4 mV) however it caused a 0.5% reduction in cell efficiency due to a reduced fill factor. It is reasonable to assume that part of the increased space-charge recombination is due to the presence of subgrain boundaries. Shunt conductance and series resistance accounted for efficiency losses of 0.3% and 0.2% respectively due to a decrease in fill-factor. The next to lowest curve in Figure 2 shows that, theoretically, the base minority carrier

diffusion length of a perfect BSF cell of this thickness and base resistivity must exceed approximately 200 μm in order to achieve a base-limited open-circuit voltage larger than experimentally observed for the large cell. The diffusion length must exceed 300 μm, which is not likely, in order to achieve a base-limited open-circuit voltage of 600 mV. Thus it is concluded that the open-circuit voltage of this cell is limited by recombination in the quasi-neutral base due to both base resistivity and minority carrier diffusion length limitations. This conclusion is consistent with results in 2 Ω-cm single crystal silicon solar cells [15].

The extent of this base recombination due to an approximately 8% area containing subgrain boundaries was calculated from the measured effective diffusion length of 80 μm in this region and equations (2) or (3). The interesting result is that approximately 40% of the total quasi-neutral current results from an region comprising approximately 8% of the cell area. This emphasizes the need to eliminate these defects by modification of the crystal growth process or possibly by passivation of these defects using, for example, atomic hydrogen [30].

SUMMARY AND CONCLUSIONS

Large area (100cm^2) polysilicon solar cells having efficiencies up to 14.1% (100mW/cm^2, 25°C) were fabricated and a detailed analysis was performed to identify the efficiency loss mechanisms. The I-V characteristics of the best cell were dominated by recombination in the quasi-neutral base due to the combination of minority carrier diffusion length and base resistivity (1.7 Ω-cm). Approximately 40% of the total quasi-neutral recombination current was attributed to regions comprising approximately 8% of the total cell area containing subgrain boundaries. These subgrain boundaries substantially reduced the local effective minority carrier diffusion length which locally increases the base recombination current. By comparison, an analysis of a 16.2% small area polysilicon solar cell (4.03cm^2) indicated that the open-circuit voltage of this cell was approaching the level where recombination in the quasi-neutral emitter begins to dominate.

Further efficiency increases in large area polysilicon solar cells can be realized by an improvement in the crystal growth, and/or post-solidification processes, to reproducibly yield low resistivity material having a long, spatially uniform, minority carrier diffusion length. After a suitable reduction in the base recombination is accomplished, a further development and application of the surface passivation and emitter formation techniques, successfully demonstrated with single crystal material, should allow efficiency advances to be made.

ACKNOWLEDGEMENTS

The authors wish to express their appreciation to L. Brickman, E. Coccia, J. Culik, D. Fardig, T. Migliorini, C. Osterwald and G. Storti for their contributions to this effort and to P. Fazio for preparing this manuscript.

REFERENCES

1. A.W. Blakers, M.A. Green, S. Jiquin, E.M. Keller, S.R. Wenham, R.B. Godfrey, T. Szpitalak and M.R. Willison, IEEE Electron Device Letters, Vol. EDL-5, No. 1, 1984.

2. M.B. Spitzer, S.P. Tobin, and C.J. Keavney, IEEE Trans. Electron Devices, Vol. ED-31, No. 5, May 1984, in print.

3. M.A. Green, A.W. Blakers, Jiqun Shi, E.M. Keller and S.R. Wenham, Appl. Phys. Lett. 44 (12), June 1984.

4. G.M. Storti, Conf. Rec., 15th IEEE Photovoltaic Specialists Conf., 442, (1981).

5. G.M. Storti, S.M. Johnson, H.C. Lin, and C.D. Wang, Conf. Rec., 14th IEEE Photovoltaic Specialists Conf., p. 191, (1980).

6. S.M. Johnson, R.G. Rosemeier, C.D. Wang, R.W. Armstrong, H.C. Lin, G.M. Storti, Proc. Int. Electron Devices Meeting, p. 202 (1980).

7. S.M. Johnson, to be published.

8. R.J. Matson, K.A. Emery, and R.E. Bird, Solar Cells, Vol. 11, No. 2 (1984).

9. K.C. Yoo, S.M. Johnson, W.F. Regnault, to be published.

10. S.M. Johnson, J.C. Culik, Conf. Rec., 16th IEEE Photovoltaic Spec. Conf., 548, (1982).

11. F.A. Lindholm, J.G. Fossum and E.L. Burgess, IEEE Trans. Electron Devices, Vol. ED-26, No. 3, March 1979.

12. J.A. Minnucci, K.W. Matthu, A.R. Kirkpatrik, and A. McCrosky, in ref. [5], p. 93.

13. M.P. Godlewski, T.M. Klucher, G.A. Mazaris, and V.G. Weizer, in ref. [5], p. 166.

14. R.A. Arndt, A. Meulenberg, and J.F. Allison, in ref. [4], p. 92.

15. E.S. Rittner, A. Meulenberg, and J.F. Allison, J. Energy, Vol. 5, No. 1, 1981.

16. A. Meulenberg and R.A. Arndt, ref. [9], 348.

17. H.T. Weaver and R.D. Nasby in ref. [9], 361.

18. M.A. Green, et.al., in ref. [4], p. 1405.

19. M.A. Green, et.al., in ref. [9], p. 1219.

20. J. Culik, P. Alexander, K.A. Dumas, and J.W. Wohlgemuth, Fifth E.C. Photovoltaic Solar Energy Conference, Athens, p. 1090-1094, (1983).

21. J. Culik, K. Grimes, 17th IEEE Photovoltaic Specialists Conf., in print (1984).

22. C. Osterwald, Report No. 296, Solar Energy Research Institute, September 20, 1983.

23. L.A. Brickman, unpublished research.

24. E. Fabre, M. Mautref, and A. Mircea, Appl. Phys. Lett., Vol. 27, pp. 239-241, (1975).

25. R. Shimokawa and Y. Hayashi, IEEE Trans. Electron Devices, Vol. ED-30, No. 12, (1983).

26. E.D. Stokes and T.L. Chu, Appl. Phys. Lett., Vol. 30, No. 8, (1977).

27. J.C. Culik, unpublished research.

28. B.H. Rose, H.T. Weaver in ref. [21].

29. V.G. Weizer, C.K. Swartz, R.E. Hart, M.P. Godlewski in ref. [21].

30. C.H. Seager, D.J. Sharp, J.K.G. Panitz, and R.V. D'Aiello, J. Vac. Sci. Technol. 20, 430, 1982.

RAI-CHOUDHURY: I notice your internal quantum efficiencies around 0.4 micrometer were in excess of 80%. Would you comment on why you had such high internal quantum efficiency without the surface passivation?

JOHNSON: I think it's strictly due to our thinner junction. We have a fairly high sheet resistance of 100 ohms per square -- maybe slightly larger than that.

RAI-CHOUDHURY: What is your surface dopant concentration?

JOHNSON: I don't know. We haven't measured that.

RAI-CHOUDHURY: It's not clear why you had such high collection efficiencies. There has got to be either low emitter surface dopant concentration or somehow your surface has got to be very well passivated, because usually even if you take a single crystal material at 0.4 micrometer you see internal quantum efficiencies of about 50% to 60% at the most, and you had 80% there.

JOHNSON: All that I can say is that it may be just from the particular way we do our diffusions.

LESK: I was just wondering, there was a paper in your organization on hydrogen passivation of defects, and I was wondering if you see any passivation of the sub-grain boundary regions with hydrogen, or can you look at it closely?

JOHNSON: We haven't done that yet. Jerry Culick, who is here, will be doing that, and there is a lot of promise for passivation of those regions, because the region where you are going to get the passivation is probably at the dislocations, where you are going to get diffusion down the boundaries due to the presence of dislocation.

SIRTL: I have two questions. One is, could you briefly describe or show the crystalline features of the two top cells you were discussing? The second question is, did you -- with the same cell technique -- make solar cells from standard monocrystal like Czochralski, just to show the differences in terms of this sophisticated cell technology?

JOHNSON: Yes. For Czochralski material, for 2 x 2 cells we can get 16 1/2% - 17% without too much difficulty. For large areas, we did process a few five-inch wafers, where we cut off the edges. We started about four of them; we got two of them finally to the end. One of the cells had an open-circuit voltage of about 600 millivolts and the other one was somewhat less than that, maybe 590 or so. This is due more to processing limitations, I think. Efficiencies run in the order of 15 1/2% for the large area cells.

SIRTL: Could you describe the two samples? Was the 2 x 2 16.2% cell largely monocrystalline, or how did it look?

JOHNSON: No, the grain size was larger, and I don't have a picture of that particular cell. The grain size in that cell was probably closer to half centimeter to a centimeter or so in size. I'd say closer to about half centimeter in size. The large-area cells, optically visible grain size is still in the range of 3 to 5 millimeters. Again, it's not the optically visible size that is important to us, it's the size under a defect. That's where we see these small-grain regions and sub-grain regions.

QUESTION: I'd like to follow up on that. Your 4 cm^2 cell had very good characteristics; do you have any feeling what is the percentage of grain boundaries? What kind of grain boundaries? Earlier you called it 8%.

JOHNSON: Oh, subgrains in that particular cell. We did not want to destroy it, naturally, but I would estimate subgrain boundaries in that particular cell were very minimal. I would say very few are in that region. For small-area cells you have the luxury of choosing good areas out of a large area. For large-area cells you have to take what the material gives you.

RAO: It's interesting that you have this 8% of the material having sub-grain boundaries, and you showed some nice pictures of that. Is there any way that can relate this to location and the sample where you have high density sub-grain boundaries, and do you know what happens at the subgrain boundaries? Why they are forming? Are they forming because of impurity segregation there, perhaps?

JOHNSON: Impurity segregation would be difficult for us to measure. Someone like Larry Kazmerski could probably measure it relatively easily. What we have found is that the electrical activity of grain boundaries is associated with dislocations at the interface. First-order twins, which do not need dislocations to make up the orientation difference, are rarely electrically active. Second-order twin boundaries can have regions that fit together coherently; there's no dislocations needed. They are all relatively active electrically. Small-angle boundaries that are totally compressed at this location are always found to be electrically active. We have always seen that to be so. Whether it's impurities, atmosphere being formed around these dislocations causing their recombination, is not very clear, but as we have seen, a lot of the people have talked about low-temperature work. It's not very straightforward why dislocations are electrically active. People have looked at this but whether it's impurities or the poor structure of the dislocation -- but again, we believe that the recombination at the grain boundary is associated with dislocation, whether it's impurities there or the natural structure of the dislocation itself.

DYER: Mine is mainly a comment, and it is in response to Rai-Choudhury's remark earlier, on how come you have this higher quantum efficiency and so forth? It just recalls to me a chemical monkey wrench that I want to throw into this whole business: that is, the chemical processing of the early slice is very important. If you thin the slice with hydroxides and then if you texture it with dilute hydroxides there are some things that will plate out of solution. For example, iron plates out of solution. If you don't do anything to remove that before you diffuse, then you

would drive iron into the emitter, and so forth, and I don't think that would be very good for the device. So, I just want to remind people of this, and of course if you are using acid cleanups, acids plate gold and copper out of solutions; you have to guard against the buildup of these materials and then replating them out. They are also bad. Just to mention this as possible effect on the V_{OC} that earlier in the meeting someone pointed out was slightly lower from texturing.

BICKLER: I'd like to comment on the origin of some of these stresses at the corners of the grain boundaries. I think it would be valuable if you did a thorough study on grain orientation from the freezing point of silicon. I'm sure the stresses you mentioned from the crucible are probably minor by the time you get in a few grains and it may submit itself to an analysis. Since you get a dimension change and different directions it may focus that force, that strain at those stress points.

DYER: It may be this, the changes in thermal gradient in the ingot, which are not nearly as well controlled as material like Czochralski, that we are getting. Now, Yoo at Texas Instruments has done a lot of looking at the origin of these stresses and what the effect is on different grain orientations. The approach that he has taken is that if you assume a particular stress direction due to thermal stresses, just based on how the ingot is going to cool, what is the resolved shear stress on the grains of different orientation? So if you have a grain in the right orientation you are going to get a very large shear stress on that particular grain and you are going to get a slip.

BICKLER: The analysis that I am talking about would be isothermal cooling, if such a thing, theoretically, exists. There still would be a differential expansion as a function of grain orientation. You could analyze that after the fact. You could look at these samples that you show pictures of and see if, in fact, there is any stress or strain.

HANOKA: I just want to follow up and try get it clear. What you are saying, in effect, is that the dislocations that are electrically active and giving you a problem are due to thermal stress. And if that's so, it's basically the same distinction then that Schwuttke made yesterday also with web, with only the stress locations that seem to be electrically troublesome. Is that right?

DYER: No, what I was saying was that the sub-grain boundaries themselves seem to be indications that they are formed from stress in the ingot. In other words, the collation of the dislocations there. When they are in a particular boundary, then their nature is very difficult to determine. We have always seen the boundaries to be electrically active. Some of the dislocations in the material, however, we only saw at low temperature. Whether they are formed from stress or they have grown into dislocations I really can't say. So we see some dislocations electrically active, some are not. I have not made a clear distinction.

QUESTION: A lack of clear contrast at room temperature does not mean that they are not adversely affecting you, though. We have seen crystal samples that have we have stressed in the JPL program. Those two pictures that I

showed yesterday: you have difficulty sometimes seeing these dislocations that you formed by stressing at room temperature. But they do affect the diffusion length, so just looking for contrast can be a little deceptive. You have to be careful without having any absolute measure of what the real lifetime or diffusion length is.

QUESTION: If you don't see a contrast at a particular defect, I would say that at room temperature it's not strongly electrically active, unless you have such a high density of defects that you can't tell the difference between the various contrasts. The contrast you see for dislocation depends on the recombination efficiency at the particular dislocation and also on the diffusion length in the surrounding material. The surrounding material is limited by impurities or point defects or some other defect; you may see a very low contrast. It may not be indicative of what's happening at dislocations. It may be the bulk material around it.

QUESTION: I generally would agree with that. But I still think one has to be careful, though. If you don't see contrast, you can't state absolutely that you don't have dislocations and that it's not affecting your lifetime.

JOHNSON: Well, I agree. I wouldn't want to say anything absolutely about it. I made a statement that if we don't see that they are not a dominating factor as far as efficiency is concerned, I wouldn't argue that they are not a factor at all.

MILSTEIN: I would comment on the two previous discussions. It is all well and good to understand how the stress interacts in causing dislocations and things of that nature; however, I think the problem that really needs to be addressed is what does one do about controlling it. In that sense, that's really the crux of what you are addressing.

JOHNSON: That is the crux of why we are spending a lot of time figuring out what forms these particular defects. We would like to tailor our particular thermal environment so as not to produce these in the as-grown crystal rather than have to try to passivate them later.

ILES: You are saying you are working on a polycrystalline material, so by definition you have, I take it, grain boundaries and sub-grain boundaries. What I would like you to comment on is what you were planning to do in the near future to improve the lifetime or the diffusion length, and some feel for what kind of a number you expect in some given time frame. Would you like to comment on that?

JOHNSON: I certainly cannot give you a number of what I would expect. What we would like to look at in more and more detail is why our lifetime does drop off as a function of dopant density, to try to determine where the actual limitations are, and it's very important to try to overcome the technological limitation of the material. Try to get to lower resistivity. So we are looking at that particular area right now. I don't have a feel for what I could say if we cast silicon sheet having resistivity of 0.5-ohm centimeters -- that we would still expect our diffusion length to be 150 micrometers. I have no basis to make a judgment.

ILES: The reason I asked that question is you have now 3.2 ohm centimeters between your float zones. Everybody's working on it and getting the diffusion length hit and miss; some crystals have it, most of them don't. What kind of ultimate limits can we gain in efficiency? If somebody has that number, and would like to comment on it?

QUESTION: I'd like to make a comment on that. It is that we know relatively well that our efficiency losses are due to the structural defects, such as grain and sub grain boundaries. We can minimize the sub-grain boundary density; that can be controlled. Independent of that, there is a problem with inter-grain minority carrier diffusion, which is related to the doping density. It's seen in Czochralski material, not seen in float-zone, in that particular area that we are looking at, and it's something that's independent of the fact that there are grain and sub-grain boundaries around. You can separate the two, but it may not be separate from the actual method that we grow the crystal. It may be, or it looks to be, inherent in Czochralski, and I hope there are some improvements down the line. I really can't say what they would be at this time.